Nuclear Physics A559 (1993) 253–265
North-Holland

NUCLEAR
PHYSICS A

Structure of intermediate states in the photoexcitation of the ^{89}Y isomer *

M. Huber, P. von Neumann-Cosel, A. Richter, C. Schlegel, R. Schulz
Institut für Kernphysik, Technische Hochschule Darmstadt, D-64289 Darmstadt, Germany

J.J. Carroll, K.N. Taylor, D.G. Richmond, T.W. Sinor, C.B. Collins
Center for Quantum Electronics, The University of Texas at Dallas, Richardson, TX 75083-0688, USA

V. Yu. Ponomarev
Laboratory of Theoretical Physics, Joint Institute for Nuclear Research, Dubna, Head Post Office, P.O. Box 79, Moscow, Russian Federation

Received 20 May 1992
(Revised 19 February 1993)

Abstract

Resonant photon scattering off ^{89}Y was investigated in a measurement of the ^{89}Y^{m} excitation function for bremsstrahlung endpoint energies $E_0 = 2$–5 MeV and in a nuclear-resonance-fluorescence experiment with $E_0 = 5$ MeV. The results are compared to a quasiparticle–phonon model calculation. Besides a well-known single-particle M1 transition at low energies, the photoexcitation spectrum is governed by transitions to states built by coupling of the dominant $p_{1/2}$ hole ground-state configuration to collective quadrupole phonons in the neighbouring ^{90}Zr. The detailed decay cascade to the isomer reproduces the experimental finding of only two intermediate states with about equal strength and explains the suppression of other possible transitions due to the nature of the particular E1 matrix element. The theoretical isomer branching ratios are small compared to the experiment, but depend critically on details of the model.

Key words: NUCLEAR REACTIONS ^{89}Y$(\gamma, \gamma')^{89}$Y^{m}; $E_0 = 2$–5 MeV; ^{89}Y(γ, γ'), $E_0 = 5$ MeV. Deduced ground-state and isomer activation transition strengths; $t_{1/2}$. Quasiparticle–phonon model calculations.

* Work supported by the German Federal Minister for Research and Technology (BMFT) under contract number 06DA641I and by the Department of Defense through the Naval Research Laboratory.

1. Introduction

The photoactivation of isomers has recently attracted considerable interest [1–5]. These studies have been motivated by several sources of interest. It has been proposed to use the population or depopulation of isomers by resonant photoabsorption as the basic mechanism for driving a γ-ray laser [6]. For feasibility studies, a much improved experimental data base is needed. Photon coupling between ground state (g.s.) and isomer plays an important role in nuclear astrophysics. As examples, photoactivation [7] of ^{176}Lu and the depopulation [1] of ^{180}Ta^{m} provide critical tests of the present understanding of the s-process element production [8,9]. An understanding of the nuclear structure of intermediate states (IS) responsible for the isomer feeding is not only of interest by itself, but also a prerequisite for progress in the above-described problems.

Most experimental photoactivation work has concentrated either on the low-energy area (see e.g. refs. [10,11] and references therein) $E \leqslant 2$ MeV, or on the giant resonance region [12–14], where the statistical γ-decay properties and the competition with other emission channels can be tested. The work described in refs. [1–5] focused on the energy region in between and produced a number of unexpected results, viz. very large integrated cross sections (ICS) in heavy-deformed nuclei implying considerable K-mixing at low energies [15], a threshold of ICS at excitation energies $E_x = 2.5$–3 MeV and a close correlation of absolute magnitudes of isomer population with the g.s. deformations [5].

A first attempt to reach a detailed understanding of the IS nuclear structure was made in the investigation of ^{115}In. Here, photoactivation and complementary nuclear-resonance-fluorescence (NRF) experiments were performed and the combined information turned out to be a powerful tool to constrain microscopic-model descriptions [4]. In the present work we have extended this combined experimental method to another example, ^{89}Y^{m}. The isomeric transition is of M4 type $\frac{1}{2}^- \rightarrow \frac{9}{2}^+$, but complementary to the ^{115}In case, ^{89}Y has a $J^\pi = \frac{1}{2}^-$ g.s. and a $J^\pi = \frac{9}{2}^+$ isomer ($E_{iso} = 0.909$ MeV). It provides an interesting case because of its semimagic nature. The reduced configuration space should facilitate the identification of the important nuclear structure aspects. Furthermore, additional information from spectroscopic studies with a variety of methods is available [16] up to relatively high excitation energies. Photoactivation of ^{89}Y^{m} was observed in the survey of ref. [3] and the yields turned out to be very small compared to other isomers in this mass region.

The results are compared to calculations with the quasiparticle–phonon model [17]. It has already been successfully applied [18] to explain the structure of IS in the photoactivation of ^{81}Br. The properties of the the ^{89}Y low-energy spectrum have been tested in a variety of other models [19–22], but the study of electromagnetic transitions has been restricted to the lowest states only.

2. Experiments and data analysis

The experiments were performed with the 10 MeV injector of the superconducting continuous-wave electron accelerator S-DALINAC in Darmstadt [23]. Fig. 1 displays the experimental area for both measurements in more detail. The electron beam traversed through a 100 μm Al exit window and impinged on a rotating 3 mm Ta converter disk for bremsstrahlung production. The electron-beam alignment could be sensitively monitored with the dose delivered to an ionization chamber 2 m downstream which is shielded against background radiation and covers only 12 mrad around 0°.

2.1. Nuclear-resonance-fluorescence experiment

For the NRF experiment, a metallic Y powder target of 2.55 g sealed in a 0.1 mg/cm^2 polyethylene foil was placed behind the 60 cm lead collimator which has a conical opening. The bremsstrahlung converter was moved to the position close to the collimator entrance indicated in fig. 1. The collimator defines a beam spot of 2.5 cm^2 at the target position. The resonantly scattered photons were detected with a Ge(Li) and a HPGe detector, both 150 cm^3, placed at 90° and 127°, respectively, relative to the beam axis. In the present experiment, only the 127° diode was used (see sect. 3). A graded shield of 9 mm Pb + 5 mm Cu was placed between target and detector in order to suppress the strong nonresonant low-energy background. Data were taken at $E_0 = 5$ MeV with a typical average current of 25 μA. The total measuring time was 32 h.

The energy calibration and relative efficiency of the Ge detector were determined off line with a ^{56}Co source with a geometry identical to the target. During the measurement, thin disks of 1.05 g Al were sandwiched around the yttrium

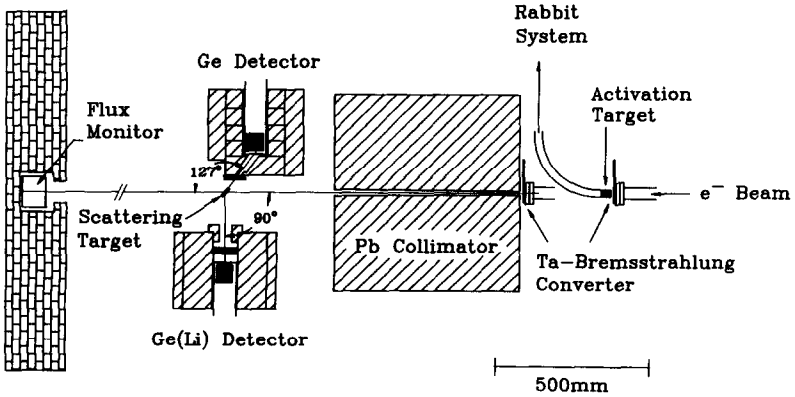

Fig. 1. Schematic, but in-scale view of the experimental area for nuclear resonance fluorescence and photoactivation studies. Note the different positions of the bremsstrahlung converter (close to the collimator for NRF) for the two types of experiments.

target. In ^{27}Al a number of extremely well-determined transitions [24] are excited in the energy region of interest and serve as standards for the determination of the total photon flux.

The shape of the bremsstrahlung spectrum was taken from a Monte Carlo calculation with the code EGS4 [25]. From fig. 1 it is obvious that the experimental geometry is simple and reliable results from the Monte Carlo calculations can be expected. The calculated spectral shapes compare very well [26,27] to the results for strong transitions in ^{27}Al and ^{11}B which are commonly used as standards. Further details of the data analysis are given in ref. [26].

From the line contents of identified transitions one obtains the ICS of the g.s. transitions $(\sigma\Gamma)_0^i$ which are related to the characteristic properties of the excited state i by

$$(\sigma\Gamma)_0^i = \pi^2 \left(\frac{\hbar c}{E_i}\right)^2 \frac{2J_i + 1}{2J_0 + 1} \frac{(\Gamma_0^i)^2}{\Gamma} W(\Theta). \tag{1}$$

Here, J_0 and J_i are the spins of the g.s. and excited state, respectively, Γ_0^i is the partial width directly to the g.s., Γ is the total width and E_i is the energy of the transition. The angular distribution $W(\Theta)$ accounts for the nonisotropic decay which depends on the multipolarity (dipole/quadrupole) and the mixing ratio δ of E2/M1 transitions.

2.2. *Isomer activation experiment*

The experiment was performed as close as possible to the bremsstrahlung converter in order to maximize the photon flux. The target consisted of an Al cylinder (diameter 1.4 cm, height 2.7 cm, walls 0.1 cm) filled with 4.8 g of YF3 powder. The cylinder was aligned to the beam direction with the front side in a distance of 1.3 cm to the converter. The sample was typically irradiated for a time duration of two half-lives ($t_{1/2} = 16.06$ s) and then transported with a high-compression rabbit system to a 3.5″ NaI bore hole detector outside of the accelerator hall. Typically 5 to 9 cycles were performed per electron endpoint energy. Details of the measurement with this shuttle system are described in refs. [5,28].

The absolute efficiency of the NaI detector was calculated with a Monte Carlo program which included the geometry of target cylinder and detector, the nonuniform distribution of activation over the length of the target and the self-absorption of the signature transition in the target material.

Following the method described in ref. [5], ICS for the states populating the isomer can be derived from the yields and the photon spectral intensities which were taken again from EGS4 calculations. The integrated cross sections $(\sigma\Gamma)_{iso}^i$

are related to eq. (1) by

$$(\sigma\Gamma)^i_{\mathrm{iso}} = \pi^2\left(\frac{\hbar c}{E_i}\right)^2 \frac{2J_i+1}{2J_0+1}\frac{\Gamma^i_0\Gamma^i_{\mathrm{iso}}}{\Gamma} = (\sigma\Gamma)^i_0 \frac{\Gamma^i_{\mathrm{iso}}}{\Gamma^i_0 W(\Theta)}. \tag{2}$$

Here, Γ^i_{iso} represents the sum of all partial widths of level i which decay to the isomer, either directly or via a cascade.

The validity of the data analysis procedures was tested with a measurement of ^{115}In. It was shown in ref. [4] that the isomeric yield below 2.8 MeV provides an absolute calibration of the total photon flux, since all activation levels are completely characterized in the literature [29]. The present results agree within 5% with those of ref. [4], which were measured in a completely different geometry with a thin disk target, as well as with the 6 MeV endpoint energy result of ref. [3].

3. Results and discussion

3.1. Nuclear resonance fluorescence of ^{89}Y

A (γ, γ') spectrum taken at an endpoint energy $E_0 = 5$ MeV is displayed in fig. 2. Except those levels marked as Al calibration lines, all visible transitions are assumed to be ^{89}Y g.s. transitions. The observation of transitions to excited states can be excluded in the present case. Since NRF is restricted to dipole or quadrupole excitations, the lowest level which could be effectively populated would be at 1.507 MeV. Because of the correspondingly reduced γ-energy, such a transition is lost in the Compton background which rises exponentially towards lower energies.

A summary of all observed transitions is given in table 1 together with the available information [16] on spins and g.s. branching ratios. In cases where both quantities are known, the resulting half life is presented in the last column. For previously unknown levels, the partial g.s. width is given as $g\Gamma_0^2/\Gamma$ with $g = (2J+1)/(2J_0+1)$.

Unlike the case of even–even nuclei where a two-point angular distribution allows a clear distinction between dipole and quadrupole transitions [26] the possible angular distributions in an odd–even nucleus are much more isotropic. Therefore, only measurements with the 127° detector which has a more favourable peak-to-background ratio were evaluated. For the angular correlations of ^{89}Y g.s. transitions $\frac{1}{2} \rightarrow \frac{1}{2}$, $\frac{3}{2}$, $\frac{5}{2} \rightarrow \frac{1}{2}$ the value of $W(\Theta)$ at 127° averaged over the detector solid angle varies by less than 15% from $W(\Theta) = 1$. Thus, the $W(\Theta)$ factor is omitted and for previously unknown levels an additional systematic error should be included. For an assigned $\frac{5}{2}^-$ spin, the values in table 1 are corrected with a factor $W(\Theta) = 0.856$. In the case of a $\frac{3}{2}^-$ state, the maximum deviation from unity for an arbitrary E2/M1 mixing ratio is less than 4.5%.

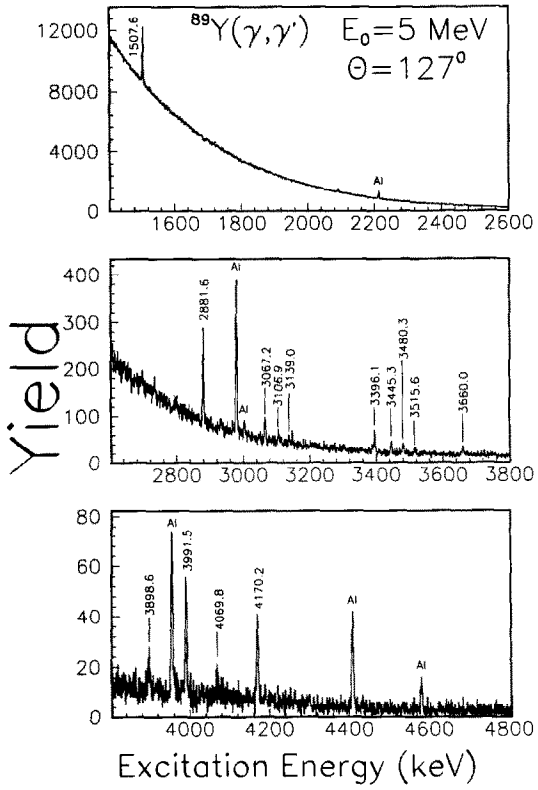

Fig. 2. Spectrum of the $^{89}Y(\gamma, \gamma')$ reaction at an endpoint energy $E_0 = 5$ MeV.

The strongest transition observed in NRF is to a state at 1.508 MeV which has $J^\pi = \frac{3}{2}^-$. Its almost pure $p_{3/2}$ hole character is well established in single nucleon pick-up [30] and (e, e′) reaction [31,32] studies. In an early (γ, γ') experiment [33] a total width $\Gamma = 22(3)$ meV was observed which compares favourably with the present value.

The 2.881 and 3.067 MeV levels correspond to M1/E2 transitions. From a combination of the $L = 1$ result in the (^{3}He, d) reaction [34] and $L = 2$ from inelastic (p, p′) and (n, n′) scattering [35,36], $J^\pi = \frac{3}{2}^-$ is clear. Refs. [37,38] show that the 2.881 MeV state decays to the g.s. with a branching ratio $b_0 \simeq 1$. Including the results from subsect. 3.2, we infer $b_0 = 0.96$.

The 3.107 and 3.139 MeV states are likely $J^\pi = \frac{5}{2}^-$ candidates. The excitation of the 3.139 MeV state in the present experiment is very weak at the threshold of the detection sensitivity. It is, however, of interest because of its significant branch [37,38] into a cascade to the isomer. It is noted that the B(E2) value of 145 e^2fm^4 reported in ref. [31] for the sum of the 3.067, 3.107 and 3.139 MeV levels unresolved in their (e, e′) experiment is in good agreement with the present results, if one assumes a dominant E2 transition for the $\frac{3}{2}^-$ state.

Table 1
Transitions in $^{89}Y(\gamma, \gamma')$

E_x (keV)	$(\sigma\Gamma)_0$ (eV · b)	$g\Gamma_0^2/\Gamma$ (meV)	J^π (ref. [16])	b_0 (ref. [16])	$t_{1/2}$ (fs)
1507.2 (1)	64.5 (36)		$\frac{3}{2}^-$	1.00	$23.9^{+2.5}_{-2.1}$
2881.6 (1)	19.6 (12)		$\frac{3}{2}^-$	0.96 [a]	$19.9^{+2.1}_{-1.9}$
3067.0 (3)	8.2 (17)		$\frac{3}{2}^-$	1.00	$45.0^{+1.5}_{-1.1}$
3106.9 (6)	4.0 (22)		$\frac{5}{2}^-$	0.87	100^{+130}_{-35}
3139.0 (5)	2.9 (11)		$\frac{5}{2}$	0.78	110^{+70}_{-30}
3396.1 (3)	11.7 (19)	35 (6)			
3445.3 (3)	5.8 (9)	18 (3)			
3480.3 (5)	6.8 (24)	21 (8)			
3515.6 (6)	2.4 (11)	8 (4)	$\frac{3}{2}^-, \frac{5}{2}^-$		
3660.0 (5)	6.7 (18)	23 (6)			
3898.6 (5)	6.1 (12)	24 (5)			
3991.8 (3)	22.4 (25)	93 (10)	$\frac{3}{2}^-, \frac{5}{2}^-$	0.95 [b], 1.00 [c]	$9.3^{+1.1}_{-1.0}$ [b], $12.6^{+1.6}_{-1.3}$ [c]
4069.8 (8)	1.0 (6)	4 (3)			
4170.2 (4)	25.5 (31)	115 (14)	$\frac{3}{2}^-, \frac{5}{2}^-$	0.95 [b], 1.00 [c]	$7.5^{+1.0}_{-0.8}$ [b], $10.1^{+1.5}_{-1.1}$ [c]

[a] Isomeric branching ratio from subsect. 3.2.
[b] If $J^\pi = \frac{3}{2}^-$ with isomeric branching ratios from subsect. 3.2.
[c] If $J^\pi = \frac{5}{2}^-$

The strong 3.992 and 4.108 MeV states are again observed in inelastic nucleon scattering as $L = 2$ states. From the available data one cannot distinguish between $J^\pi = \frac{3}{2}^-$ and $\frac{5}{2}^-$. A g.s. branching ratio of $b_0 \simeq 1$ can be deduced for both states from refs. [37,38].

No candidate for an E1 transition is seen in the (γ, γ') data. For those $\frac{3}{2}^-$ levels which are simultaneously observed in the (p, p') and (n, n') experiments, dominant E2 transition strength is suggested from the collective character of inelastic nucleon scattering reactions.

3.2. *Photoactivation of $^{89}Y^m$*

The isomer yield resulting from the bremsstrahlung irradiation is shown in fig. 3 as a function of the endpoint energy. Up to 2.875 MeV no isomer activity is detected. Towards higher energies, breaks of the excitation function are clearly visible just below 3 and around 4 MeV. The solid line results from a calculation assuming IS at 2.9 and 4.0 MeV with the ICS given in table 2.

The good agreement with the energies of states excited strongly in the (γ, γ') reaction together with the model results described in sect. 4 clearly suggests that the 2.881 MeV state is the first IS. The ICS of the weakly excited 3.139 MeV level is in any case too small to explain the first break. Because of the small number of data points the energy of the second IS is more uncertain and we cannot

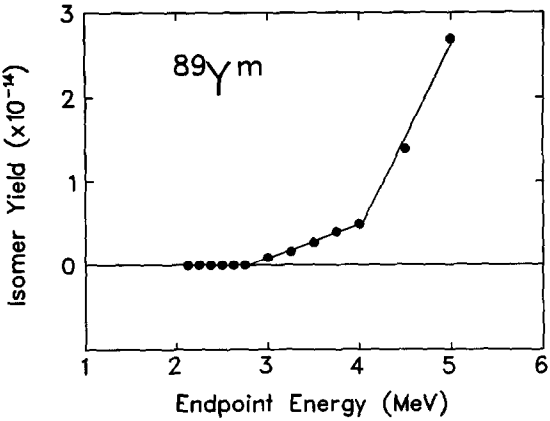

Fig. 3. The ^{89}Y isomer yield as a function of the bremsstrahlung endpoint energy. The solid line represents calculated values [5] using the intermediate states of table 2.

distinguish whether the 3.992 or the 4.170 MeV level provides the isomer population.

Compared to typical values of ICS in the energy region 2–4 MeV observed in refs. [1,2,4,5], the isomer population in ^{89}Y is weak. This finding is also in qualitative agreement with the yield values at 4 and 6 MeV deduced in ref. [3]. While the average $(\sigma\Gamma)_0$ strength is even slightly higher than observed for ^{115}In in ref. [4], the isomeric ratio $\Gamma_{iso}/\Gamma_0 + \Gamma_{iso}$ is about an order of magnitude smaller.

4. Quasiparticle–phonon model calculations

4.1. Details of the calculations

To understand the structure of states observed in the present experiments microscopic calculations within the quasiparticle–phonon model have been performed. A detailed description of treating odd nuclei within this theoretical framework can be found in ref. [17].

Table 2
Intermediate states in the photoactivation of $^{89}Y^m$

E_x (MeV)	$(\sigma\Gamma)_{iso}$ (eV · b)
2.9 (1)	0.8 (1)
4.0 (2)	1.2 (5)

The present calculations have been performed with the wave function

$$\Psi_\nu(JM) = C_J^\nu \left\{ \alpha_{JM}^+ + \sum_{\lambda\mu i} D_j^{\lambda i}(J\nu) \left[\alpha_{jm}^+ Q_{\lambda\mu i}^+ \right]_{JM} \right\} \Psi_0 \tag{3}$$

of the ground or excited states with angular momentum J and projection M. In this equation α_{jm}^+ is a quasiparticle creation operator, $Q_{\lambda\mu i}^+$ is a phonon creation operator with the momentum λ, projection μ and the RPA-root number i, Ψ_0 is the ground-state wave function of the even–even core and ν is the number within a sequence of states with given J^π. For phonons we consider both collective, such as 2_1^+ or 3_1^-, and pure two-quasiparticle excitations of the core.

Numerically, equations for ^{89}Y have been solved by use of the computer code PHOQUS [39]. The QPM effective hamiltonian includes an average field, pairing interaction and residual interaction between quasiparticles. The average field was treated by a Woods–Saxon potential with parameters from ref. [40]. Parameters of the residual interaction were adjusted to reproduce the experimental position and the $B(E\lambda)$ values of the 2_1^+ and 3_1^- states for ^{90}Zr while dealing with hole excitations and for ^{88}Sr in case of particle excitations. Natural-parity phonons with $\lambda^\pi = 1^- - 6^+$ have been included in the second term of the wave function eq. (3). We have taken into account "quasiparticle ⊗ phonon" configurations up to an excitation energy of 12 MeV. Nevertheless, actual calculations show that only collective 2^+ phonons play an important role in description of photoexcitation of states up to 5 MeV, since the interaction between different phonon configurations is not strong in this nucleus.

4.2. Comparison to nuclear-resonance-fluorescence results

The calculated (γ, γ') excitation strength is presented in fig. 4 together with the experimental $(\sigma\Gamma)_0$ data. In the QPM only 6 sizeable transitions are found below 4.5 MeV. Due to the restriction of the model space to one-phonon coupled states the degree of fragmentation is less than indicated by the experimental results. However, since higher phonon configurations do not contribute additional photoexcitation strength, the main features of the (γ, γ') results can already be explained in the one-phonon approximation.

The two lowest states in the calculation at 1.540 and 1.838 MeV correspond to the well-known lowest $J^\pi = \frac{3}{2}^-$ and $\frac{5}{2}^-$ states which have been shown [30] to be of dominant $p_{3/2}$ and $f_{5/2}$ single-hole structures, repectively. The model result for the $\frac{3}{2}^-$ level $(\sigma\Gamma)_0 = 70.2$ eV · b is in excellent agreement with experiment. The $\frac{5}{2}^-$ state was not observed in the experiment. One can calculate from the g.s. transition strength of $(\sigma\Gamma)_0$ 4.67 eV · b from the data available [16] and show that the experimental count rate is smaller than the background fluctuations.

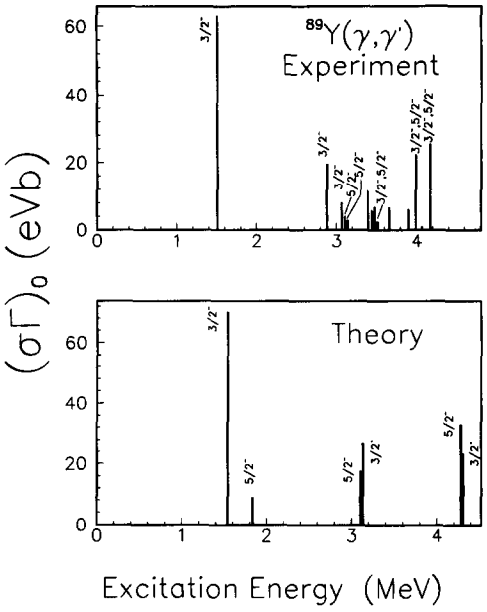

Fig. 4. Comparison of the experimental integrated cross sections $(\sigma\Gamma)_0$ of g.s. transitions in the $^{89}Y(\gamma, \gamma')$ reaction with QPM calculations. The experimental spin assignments are from ref. [16].

The next transitions are in two groups of nearly degenerate levels which result from the coupling of the g.s. configuration to the lowest collective phonons [41] in the neighbouring even–even nucleus ^{90}Zr, i.e. dominant $[p_{1/2} \otimes 2^+_{1,3}]_{3/2^-,5/2^-}$ structure. The near degeneracy is a result of the neglect of more complex configurations and would probably be removed if one included two-phonon states.

The 3.147 MeV, $J^\pi = \frac{3}{2}^-$ model state corresponds to the experimental 2.881 MeV and probably the 3.067 MeV state. The magnitudes of ICS support this assignment. The $\frac{5}{2}^-$ model state can be reasonably compared to the more fragmented experimental strength up to 3.5 MeV. The levels resulting from coupling to the 2^+_3 state can be identified with the experimental levels at 3.992 and 4.170 MeV.

The structure of these states implies that the phonon transitions are responsible for the (γ, γ') strength. The general dominance of collective E2 strength in the NRF data explains the close correspondence to inelastic nucleon scattering results discussed in sect. 3.

4.3. Comparison to isomer activation results

Since the relevant excitation spectrum is entirely explained assuming M1 and E2 transitions, for a total M4 transfer the intermediate-state decay must proceed in a two-step cascade including an E1 transition for the parity change. Fig. 5 presents a calculated level scheme according to this condition. The first step in the cascade to

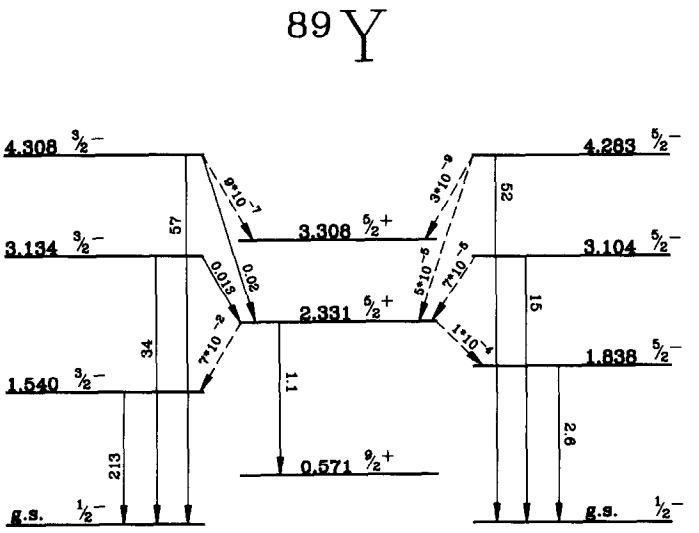

Fig. 5. Selected scheme of levels and partial decay widths from the QPM results for ^{89}Y. The graph is restricted to states relevant to the photoexcitation of $^{89}Y^{m}$. The levels are split in $J^{\pi} = \frac{3}{2}$ states in the left column, $J^{\pi} = \frac{5}{2}^{-}$ states in the right column and positive-parity states in the middle. The decay widths are given in meV. Weak transitions are denoted by dashed lines.

the isomer is limited to $\frac{5}{2}^{+}$ final states and two are found in the energy region considered.

While the g.s. partial widths are comparable for $\frac{3}{2}^{-}$ and $\frac{5}{2}^{-}$ states, large differences are observed in the population of the $\frac{5}{2}^{+}$ states. The decay to the higher model state at 3.308 MeV is extremely weak due to its almost pure $[p_{1/2} \otimes 3_1^-]_{5/2^+}$ character which restricts to a strongly suppressed $2_1^+ \rightarrow 3_1^-$ phonon transition. The decay widths of the $\frac{5}{2}^{-}$ states to the lower $\frac{5}{2}^{+}$ state are much weaker compared to the transitions from the $\frac{3}{2}^{-}$ levels, since the reduced E1 transition matrix elements are about an order of magnitude smaller. The lowest $\frac{5}{2}^{+}$ state is strongly coupled to the isomer via a large $[g_{9/2} \otimes 2_1^+]_{5/2^+}$ component in the wave function, so the transitions from the $\frac{3}{2}^{-}$ states are responsible for the isomer population. This result is in full agreement with the experimental finding of only two IS with about equal strength as well as with the deduced energies.

However, here the description depends on weak quasiparticle configurations of both, initial and final state, which are sensitive to details such as basis truncation and collectivity of phonons. This aspect of the calculations could certainly be improved by the inclusion of the "quasiparticle ⊗ 2-phonon" states where configurations like $[p_{3/2} \otimes [2_1^+ \otimes 3_1^-]_{1^-}]$ are expected to contribute. Also, an extension of the model space by summation over the principle quantum number N for the quasiparticle configuration [42] could be important.

5. Conclusions

The photoexcitation of ^{89}Y was investigated with two different methods. NRF data were measured at $E_0 = 5$ MeV and states up to excitation energies of 4.2 MeV could be identified. The $^{89}Y^m$ excitation function for $E_0 = 2$–5 MeV revealed no activity up to 2.9 MeV and only two IS were found up to 5 MeV.

The (γ, γ') transitions can be explained with a QPM calculation as the coupling of collective phonons in the neighbouring ^{90}Zr with the $p_{1/2}$ hole g.s. configuration leading to groups of $\frac{3}{2}^-$, $\frac{5}{2}^-$ states. While the total electromagnetic transition strength agrees favourably, the experimental fragmentation is underestimated due to the model's restriction to one-phonon coupled states. The omission of more complex configurations is justified for the present problem, since they do not add electromagnetic strength. Besides a well-known low-lying single particle MI transition, the excitation is governed by E2 phonon transitions.

The calculations demonstrate that the cascade needed for the activation of $^{89}Y^m$ proceeds via the lowest $\frac{5}{2}^+$ state which decays almost exclusively to the isomer. The experimental finding of only two IS at about 2.9 and 4.0 MeV is verified and the coupling to the $\frac{5}{2}^+$ state is of single particle E1 character. Due to the nature of the transition matrix elements the $\frac{5}{2}^- \rightarrow \frac{5}{2}^+$ transitions are suppressed by more than two orders of magnitude with respect to the $\frac{3}{2}^- \rightarrow \frac{5}{2}^+$ transitions. The calculated branching ratios are small compared to the experiment. However, they depend critically on weak quasiparticle components of the initial- and final-state wave functions.

One can conclude that up to energies of about 5 MeV the main features of the electromagnetic excitation as well as the decay of the excited states to the ^{89}Y isomer are now understood. The usefulness of a combination of NRF and isomer activation experiments has again been proven as a powerful method for nuclear structure studies.

We thank H.-D. Gräf and H. Weise for their great support in operating the accelerator. We are indebted to W. Ziegler for his help in the experiment. One of us (V.Yu.P.) would like to thank the members of the S-DALINAC group for their hospitality during his stay in Darmstadt.

References

[1] C.B. Collins, J.J. Carroll, T.W. Sinor, M.J. Byrd, D.G. Richmond, K.N. Taylor, M. Huber, N. Huxel, P. von Neumann-Cosel, A. Richter, C. Spieler and W. Ziegler, Phys. Rev. C42 (1990) R1813

[2] J.J. Carroll, T.W. Sinor, D.G. Richmond, K.N. Taylor, C.B. Collins, M. Huber, N. Huxel, P. von Neumann-Cosel, A. Richter, C. Spieler and W. Ziegler, Phys. Rev. C43 (1991) 897

[3] J.J. Carroll, M.J. Byrd, D.G. Richmond, T.W. Sinor, K.N. Taylor, W.L. Hodge, Y. Paiss, C.D. Eberhard, J.A. Anderson, C.B. Collins, E.C. Scarbrough, P.P. Antich, F.J. Agee, D. Davis, G.A. Huttlin, K.G. Kerris, M.S. Litz and D.A. Whittacker, Phys. Rev C43 (1991) 1238

[4] P. von Neumann-Cosel, A. Richter, C. Spieler, W. Ziegler, J.J. Carroll, T.W. Sinor, D.G. Richmond, K.N. Taylor, C.B. Collins and K. Heyde, Phys. Lett. B266 (1991) 9
[5] C.B. Collins, J.J. Carroll, K.N. Taylor, D.G. Richmond, T.W. Sinor, M. Huber, P. von Neumann-Cosel, A. Richter and W. Ziegler, Phys. Rev. C46 (1992) 952
[6] C.B. Collins, F.W. Lee, D.M. Shemwall, B.D. DePaola, S. Olariu and I.I. Popescu, J. Appl. Phys. 53 (1982) 4645
[7] N. Klay, F. Käppeler, H. Beer and G. Schatz, Phys. Rev C44 (1991) 2839;
K.T. Lesko, E.B. Norman, R.-M. Larimer, B. Sur and C.B. Beausang, Phys. Rev. C44 (1991) 2850
[8] F. Käppeler, H. Beer and K. Wisshak, Rep. Prog. Phys. 52 (1989) 945
[9] J.J. Carroll, J.A. Anderson, J.W. Glesener, C.D. Eberhard and C.B. Collins, Astroph. J. 344 (1989) 454
[10] E.C. Booth and J. Brownson, Nucl. Phys. A98 (1967) 529
[11] Á. Veres, At. Energy Rev. 18 (1980) 281
[12] Z.M. Bigan, E.L. Lazarev, V.M. Mazur and V. Sokolnyk, Sov. J. Nucl. Phys. 49 (1989) 567
[13] L.Z. Dzhilavyan, V.L. Kauts, V.I. Furman and A.Y. Chaprikov, Sov. J. Nucl. Phys. 51 (1990) 215
[14] J. Sáfár, H. Kaji, K. Yoshihara, L. Lakosi and Á. Veres, Phys. Rev. C44 (1991) 1086
[15] J.J. Carroll, C.B. Collins, P. von Neumann-Cosel, D.G. Richmond, A. Richter, T.W. Sinor and K.N. Taylor, Phys. Rev. C45 (1992) 470
[16] H. Sievers, Nucl. Data Sheets 58 (1989) 351
[17] S. Galès, Ch. Stoyanov and A.I. Vdovin, Phys. Reports 166 (1988) 125
[18] V. Yu. Ponomarev, A.P. Dubenskij, V.P. Dubenskij and E.A. Boykova, J. of Phys. G16 (1990) 1727
[19] P. Hofstra and K. Allaart, Z. Phys. A292 (1979) 159
[20] S.M. Abecasis, J. Davidson and M. Davidson, Phys. Rev. C22 (1980) 2237
[21] C.A. Heras and S.M. Abecasis, Phys. Rev. C27 (1983) 1765
[22] X. Ji and B.H. Wildenthal, Phys. Rev. C38 (1988) 2849
[23] K. Alrutz-Ziemssen, D. Flasche, H.-D. Gräf, V. Huck, M. Knirsch, W. Lotz, A. Richter, T. Rietdorf, P. Schardt, E. Spamer, A. Staschek, W. Voigt, H. Weise and W. Ziegler, Part. Acc. 29 (1990) 53
[24] P.M. Endt, Nucl. Phys. A521 (1990) 200
[25] W.R. Nelson, H. Hirayama and D.W.O. Rogers, Stanford Linear Accelarator Report 265 (1985)
[26] W. Ziegler, Dissertation, Technische Hochschule Darmstadt (1990)
[27] N. Huxel, Diploma thesis, Technische Hochschule Darmstadt (1992)
[28] M. Huber, Diploma thesis, Technische Hochschule Darmstadt (1992)
[29] J. Blachot and G. Marguier, Nucl. Data Sheets 52 (1987) 565
[30] A. Stuirbank, G.J. Wagner, K.T. Knöpfle, L.K. Pao, G. Mairle, H. Riedesel, K. Schindler, V. Bechtold and L. Friedrich, Z. Phys. A297 (1980) 307
[31] S.P. Fivozinskij, S. Penner, J.W. Lightbody Jr. and D. Blum, Phys. Rev. C9 (1974) 1533
[32] J.E. Wise, F.W. Hersman, J.H. Heisenberg, T.E. Milliman, J.P. Connelly, J.R. Calarco and C.N. Papanicolas, Phys. Rev. C42 (1990) 1077
[33] W.J. Alston III, H.H. Wilson and E.C. Booth, Nucl. Phys. A116 (1968) 281
[34] G. Vourvopoulos, R. Shoup and B.A. Brown, Nucl. Phys. A174 (1971) 581
[35] J. Hulstman, H.P. Blok, J. Verburg, J.G. Hoogteyling, C.B. Nederveen, H.T. Vijlbrief, E.J. Kapstein, S.W. Milo and J. Blok, Nucl. Phys. A251 (1975) 269
[36] Y. Yiming, C.E. Brient, R.W. Finlay, G. Randers-Pehrson, A. Marcinkowski, R.C. Taylor and J. Rapaport, Nucl. Phys. A390 (1982) 449
[37] C. Nardelli, P. Pavan and G. Tornielli, Lett. Nuovo Cimento 38 (1983) 129
[38] C. Budtz-Jørgensen, P. Guenther, A. Smith, J. Whalen, W.C. McMurray, M.J. Renan and I.J. van Heerden, Z. Phys. A319 (1984) 47
[39] Ch. Stoyanov and C.Z. Khuong, Preprint JINR Dubna P-4-81-234 (1981)
[40] V. Yu. Ponomarev, V.G. Soloviev, Ch. Stoyanov and A.I. Vdovin, Nucl. Phys. A323 (1979) 446
[41] P.M. Endt, At. Data Nucl. Data Tables 23 (1979) 547
[42] P. von Neumann-Cosel, A. Richter, H.-J. Schmidt-Brücken, G. Schrieder, H. Lenske, H.H. Wolter, J. Carter, R. Jahn, B. Kohlmeyer and D. Schüll, Nucl. Phys. A516 (1990) 385